



Woody biomass fly ash as a low-cost sorbent for the removal of ionic dye from aqueous solution: isotherm, kinetic modelling and thermodynamics

Lidija Čurković^{a,*}, Mirela Jukić^b, Zrinka Šokčević^a, Marijana Majić Renjo^a

^aDepartment of Materials, Faculty of Mechanical Engineering and Naval Architecture, University of Zagreb, Ivana Lučića 5, 10000 Zagreb, Croatia, Tel. +385 1 6168 183; Fax: +385 1 6156 940; email: lidija.curkovic@fsb.hr (L. Čurković), Tel. +385 1 6168 362; emails: zsokcevic@fsb.hr (Z. Šokčević), marijana.majic@fsb.hr (M. Majić Renjo)

^bAndrija Štampar Teaching Institute of Public Health, Mirogojska cesta 16, 10000 Zagreb, Croatia, Tel. +385 1 4696 259; Fax: +385 1 4678 107; email: mirela.jukic@stampar.hr (M. Jukić)

Received 20 April 2017; Accepted 27 August 2017

ABSTRACT

The main goal of this work was to investigate a possible application of woody biomass fly ash (WBFA) as a low-cost sorbent for the removal of ionic, toxic and carcinogenic diazo dye (Congo red [CR]) from aqueous solutions. Biomass fly ash is a by-product generated during mixed wood biomass combustion in the 1 MW electric power facility in Udbina, Croatia. Batch sorption experiments were carried out to evaluate the influence of experimental parameters, such as initial dye concentration, contact time and temperature on the sorption process. The experimental data were analyzed using different isotherm and kinetic models. The best fit was achieved by the Langmuir isotherm equation ($R^2 > 0.9904$). Results of the kinetic studies showed that the CR dye sorption onto the WBFA was best described by the pseudo-second-order kinetic model. The Weber–Morris intraparticle diffusion model indicated that the intraparticle diffusion is not the rate-limiting step, while the Boyd model suggested that the film diffusion might be rate-limiting. The calculated thermodynamic parameters (ΔG° , ΔH° and ΔS°) showed that the sorption of CR is feasible, spontaneous and endothermic. Experimental results confirmed that the WBFA had the potential to be utilized as a low-cost sorbent material for the removal of CR dye from aqueous media.

Keywords: Sorption kinetics; Thermodynamic; Congo red; Woody biomass fly ash

1. Introduction

Wastewater effluents from many industries, such as textile, plastic, food packaging, pulp, paper, paint, tannery, electroplating, cosmetic, printing, etc., contain several kinds of synthetic dyestuffs [1]. It is estimated that approximately 10,000 different dyes and pigments are produced commercially worldwide, with an annual production of more than 700,000 tonnes; among them nearly 60%–70% are azo dyes [2]. About 5%–10% of the dyestuffs are lost in the industrial effluents [3]. There are numerous types of dyes with 25 structural classes. The most important of them are azo

dyes. Azo dyes are characterized by the presence of one or more chromophoric azo ($R_1-N=N-R_2$) groups and aromatic rings, mostly substituted by sulphonate groups. Azo dyes are highly stable to light, heat, water, detergents, bleach and perspiration due to their resonance and π -conjugated azo bond characteristics. Azo dyes are diazotized amines coupled to an amine or phenol, with one or more azo bonds ($-N=N-$). Many of them are extremely toxic, carcinogenic, poisonous and can cause allergic reactions or pose other dangerous threats to human and animal health [4]. Therefore, the removal of synthetic dyes with azo aromatic groups from waste effluents is of significant importance for the environment. The dyes have low biodegradability and conventional biological wastewater treatment processes are inefficient in the dye removal process [5]. Therefore,

* Corresponding author.

dye wastewater is usually treated by physical and chemical methods, including electrochemical removal [6], electrochemical degradation [7], coagulation and flocculation [8], membrane separation [9], sonochemical degradation [10], photochemical degradation [11,12], photo-Fenton processes [13] and oxidation or ozonation [14].

The sorption process provides an attractive alternative treatment, especially if the sorbent is inexpensive and readily available [15]. Activated carbon is the most popular sorbent, which has been used with great success. However, activated carbon is expensive and its regeneration and reuse increase the costs. As a consequence, there is a constant search for alternative low-cost sorbents. A sorbent can be considered low-cost if it requires little processing, is abundant in nature or is a by-product or waste material from another industry. Certain non-conventional, low-cost waste products from industrial and agricultural operations, natural materials and biosorbents represent potentially alternative sorbents for dye removal. This includes orange and lemon peels [16], pine tree leaves [17], *Phoenix dactylifera* seeds [18], clays [19], rice hull ash [20], apricot stone [21], fly ash [22], *Azolla pinnata* [23], *Avena sativa* (oat) hull [24], etc., which have all been used for the removal of various dyes from wastewaters. However, new low-cost and non-hazardous sorbents are still under development.

In the present study, woody biomass fly ash (WBFA) as the low-cost and non-hazardous material was used as the sorbent for the removal of Congo red (CR) dye from its aqueous solutions. The influence of experimental parameters, such as contact time, initial CR concentrations and temperature was studied. Isotherm, kinetic and thermodynamic parameters for sorption system WBFA/CR were determined and analyzed.

2. Materials and methods

2.1. Sorbent – woody biomass fly ash

All sorption experiments were performed on biomass fly ash, by-product generated during mixed woody biomass combustion in the 1 MW electric power facility in Udbina, Croatia. The amount (wt%) of main and minor elements in fly ash biomass was determined by energy dispersive X-ray fluorescence spectrometer, EDX-800 HS, Shimadzu, Japan. Concentration (mg/kg) of trace elements in the fly ash was determined, after the microwave digestion, by the inductively coupled plasma mass spectrometry (ELAN DRC) and the atomic absorption spectrometry (AAnalyst 600, PerkinElmer, USA).

Particle-size distribution of WBFA was determined by sieving the sample on an automatic sieve shaker (model AS200 basic, Retsch, Germany) through stainless steel sieves using a stack of nested sieves (DIN/ISO 3310-1) with the following aperture size: 32, 50, 63, 125, 212 and 250 μm . The weight of each size fraction was recorded and the percentage distribution of weight in each fraction was calculated.

Fourier transform infrared (FTIR) spectra were obtained on the PerkinElmer Spectrum Two FTIR spectrometer equipped with Diamond UATR accessory. The FTIR spectra were measured in the ATR mode in the range of 4,000–450 cm^{-1} with the resolution of 2 cm^{-1} .

The morphology of the WBFA surface was examined by the scanning electron microscope (SEM), Tescan Vega TS 5136 MM.

2.2. Sorbate – Congo red dye

CR contains an azo ($-\text{N}=\text{N}-$) chromophore and an acidic auxochrome ($-\text{SO}_3\text{H}$) associated with the benzene structure (Fig. 1). The acidic diazo dye CR is a sodium salt of 3,3'-([1,1'-biphenyl]-4,4'-diyl)bis(4-aminonaphthalene-1-sulphonic acid) (C.I. No. 22120, Direct red 28, formula: $\text{C}_{32}\text{H}_{22}\text{N}_6\text{Na}_2\text{O}_6\text{S}_2$; molecular weight: 696.66 g/mol).

A stock solution of CR dye was prepared (100 mg/L) by dissolving a required amount of dye powder in deionized water. The experimental solutions of the different dye concentrations were prepared by diluting the stock solution with the suitable volume of deionized water to obtain the desired concentration ranging from 10 to 80 mg/L.

2.3. Batch sorption experiments

The sorption of CR on the biomass fly ash was investigated in the batch mode sorption equilibrium experiments. All batch experiments were carried out in 50 mL flasks containing a fixed amount of sorbent (200 mg of WBFA) with 50 mL dye solution at the known initial concentration. The flasks were agitated at the constant speed of 300 rpm in an incubator shaker. The influence of the contact time (15–240 min), the initial dye concentration (10–80 mg/L) and the temperature (15°C, 25°C and 35°C) was evaluated during the present study.

After the addition/dispersion of biomass fly ash in CR dye solutions, initial pH values of each CR dye concentration (pH 6.82–7.26) were increased up to pH 11.6 and after 240 min of sorption process increased up to pH 12.1.

The samples were collected from the flasks at predetermined time intervals for the residual dye concentration analysis. The quantity of the CR in the liquid phase remaining after the equilibration has been measured by the UV/Vis spectrophotometer (UV/Vis Cary 60, Agilent, USA) at the wavelength $\lambda = 498 \text{ nm}$. All experiments were conducted in triplicates.

In the batch equilibrium tests, the difference between the initial and the equilibrium mass concentrations of CR is used for the calculation of the quantity of CR adsorbed on the unit mass of the WBFA (q , mg CR/g WBFA), taking into consideration the data related to the WBFA weight, volume and mass concentration of the solution. The amount of CR sorbed onto the biomass fly ash was calculated from the following expression:

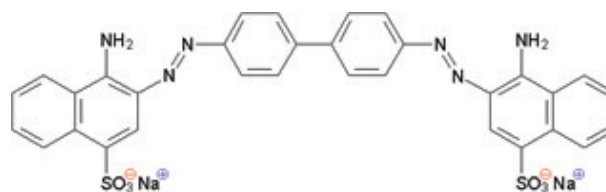


Fig. 1. Molecular structure of Congo red dye.

$$q_e = \frac{(\gamma_0 - \gamma_e) \cdot V}{m} \quad (1)$$

where q_e is the equilibrium CR concentration sorbed on the WBFA (mg/g), V is the initial volume of the CR solution used (L), m is the mass of the used WBFA (g), γ_0 is the initial concentration of the CR in the solution (mg/L) and γ_e is the concentration of the CR in the solution at the equilibrium point (mg/L).

The procedure of the kinetic sorption tests was identical to that of the batch equilibrium tests. However, the aqueous samples were taken at suitable time. The CR dye sorption at any time, q_t (mg/g), was calculated from the following equation:

$$q_t = \frac{(\gamma_i - \gamma_t) \cdot V}{m} \quad (2)$$

where γ_i (mg/L) is its initial concentration, γ_t (mg/L) is the CR concentration after the period t (min), V (L) is the solution volume and m (g) is the sorbent mass.

3. Results and discussion

3.1. Characterization of the woody biomass fly ash

The results of the chemical analysis of the investigated WBFA are presented in Tables 1 and 2.

Table 1

Main and minor elements in woody biomass fly ash (WBFA) sample (wt%)

Sample	BFA
TiO ₂	0.415
Fe ₂ O ₃	3.90
Na ₂ O	2.05
MgO	4.60
Al ₂ O ₃	2.33
SiO ₂	19.1
P ₂ O ₅	2.06
SO ₃	1.54
K ₂ O	10.2
CaO	45.9

Table 2

Concentration (mg/kg) of trace elements in woody biomass fly ash sample

Sample	BFA
Cr	76.4
Cu	89.6
Zn	102
Ni	28.0
Pb	13.1
Cd	2.38
As	3.34
Hg	0.031

The particle sizes of the WBFA were: <32 μm (2.22 wt%), 32–50 μm (9.52 wt%), 50–63 μm (2.66 wt%), 63–125 μm (22.0 wt%), 125–212 μm (37.9 wt%), 212–250 μm (8.20 wt%) and >250 μm (17.5 wt%).

The CR dye sorption on the WBFA surface was confirmed by the FTIR and SEM analysis before and after the sorption. The FTIR spectrum of CR (Fig. 2(B)) exhibits broad band centred around 3,470 cm^{-1} due to the NH₂ stretching. Strong absorption assigned to NH₂ scissoring mode is observed at 1,584 cm^{-1} . The amine group C–N stretching is observed at 1,348 cm^{-1} . Absorption bands at 1,223 and 1,064 cm^{-1} can be assigned to –SO₃[–] vibrational modes. The FTIR spectrum of WBFA (Fig. 2(A)) exhibits broad bands consistent with the determined composition of the sorbent (Table 1). The WBFA consists of the simple inorganic compounds, so unambiguous assignment of spectrum is difficult due to the significant overlapping of the bands. Nevertheless, some assumptions can be made. Broad band at 1,409 cm^{-1} and sharp band at 875 cm^{-1} can be assigned to CaO vibrational modes. Absorption band which can be associated with SiO₂ modes is observed at 1,110 cm^{-1} . The FTIR spectrum of the CR + WBFA (Fig. 2(C)) lacks most of the characteristic CR dye absorptions due to the adsorption of the dye on the adsorbent surface. The FTIR spectra (Fig. 2(C)) show that there is a slight shifting of sorbent peaks after the sorption. No new peak has been observed; indicating that no chemical bond is formed between the sorbate and the sorbent after the sorption, that is, the FTIR data confirms that the dye sorption on the sorbent is a result of the physical forces.

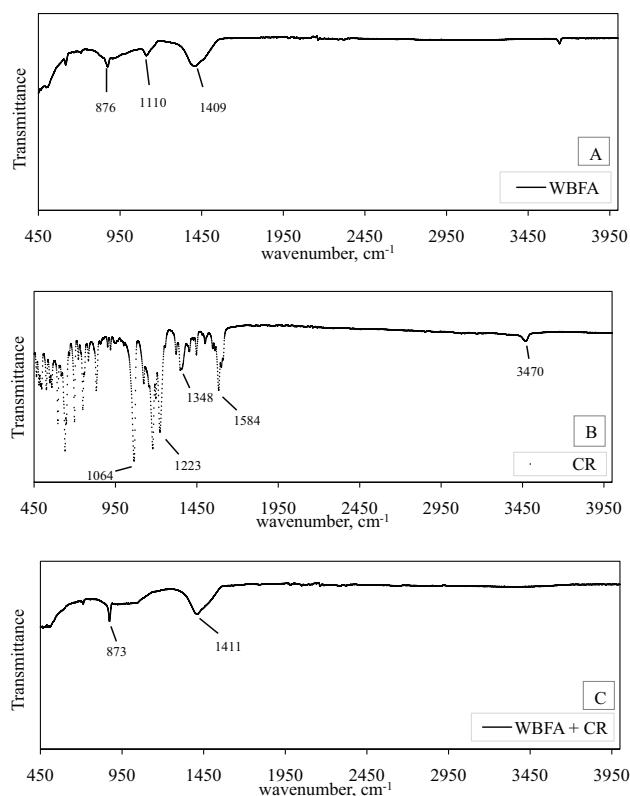


Fig. 2. FTIR spectra for (A) woody biomass fly ash (WBFA), (B) Congo red (CR) dye and (C) CR dye loaded WBFA.

The SEM micrographs of the WBFA before and after the CR sorption are shown in Figs. 3(A) and (B), respectively. The surface structure of the WBFA before the sorption is rough and porous, but after the sorption its morphology has changed – the sorbent surface is covered with dye and therefore smoother.

3.2. The effect of the contact time and the initial dye concentration

In order to establish the optimal time for the maximal removal of the CR dye by the WBFA sorbent, the removal process was studied as a function of contact time. The effect of the contact time on the dye removal from aqueous solution was investigated at the different initial dye concentration onto the WBFA sorbent. The results are presented in Fig. 4. The sorption process can be described with the following steps: the first step lasts 15–120 min and is characterized by the gradual increase in the amount of CR removed with the increasing reaction time, until the equilibrium is reached; the second step is referring to the complete saturation of the WBFA sorbent by the sorbed CR dye molecules – the plots of the three evaluated dye concentrations reached the maximum removal values at 120 min of shaking. The results show that the sorption process reached the equilibrium within 120 min. The amount of the removed CR dye increased from 4.77 to 10.1 mg/g with the increasing initial concentration of the CR dye from 20 to 60 mg/L (Fig. 4).

The effect of the different initial dye concentrations (from 10 to 80 mg/L) and the temperature (from 15°C to 35°C) on the sorption of CR by WBFA is shown in Fig. 5.

It can be seen from the plots of q_e vs. γ_e that the increase in the initial CR concentration and the temperature leads to the increase in the sorption capacity, q_e . The removal efficiency showed the opposite trend (Fig. 5): when the initial dye concentration and the temperature were increased, the dye removal efficiency was decreased. A similar trend was reported for the adsorption of CR onto tea waste [25], acid-activated red mud [26] and rubber seeds [27].

3.3. The sorption isotherm

Sorption isotherm explains the interaction between the sorbate and sorbent and is critical for the sorption process design. The Freundlich and Langmuir isotherms are the most frequently used models to describe the experimental data of sorption. In the present work, these isotherms were employed for describing the sorption process of CR on WBFA.

The Freundlich isotherm, as two-parameter model, is the earliest known relationship describing the sorption equation [28]. This empirical model can be applied to non-ideal sorption on heterogeneous surfaces as well as multisite or multi-layer sorption and can be expressed as follows:

$$q_e = K_F \cdot \gamma_e^{1/n} \quad (3)$$

where q_e is the amount of CR sorbed per unit of sorbent – WBFA (mg/g), γ_e is the concentration of CR at sorption

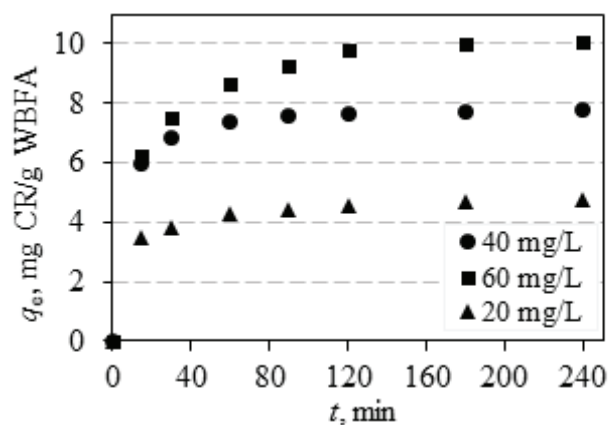


Fig. 4. Effect of contact time on Congo red dye removal by woody biomass fly ash (WBFA) at the various initial concentrations. Condition: m (WBFA) = 200 mg, V (CR) = 50 mL, agitation speed = 300 rpm, T = 25°C.

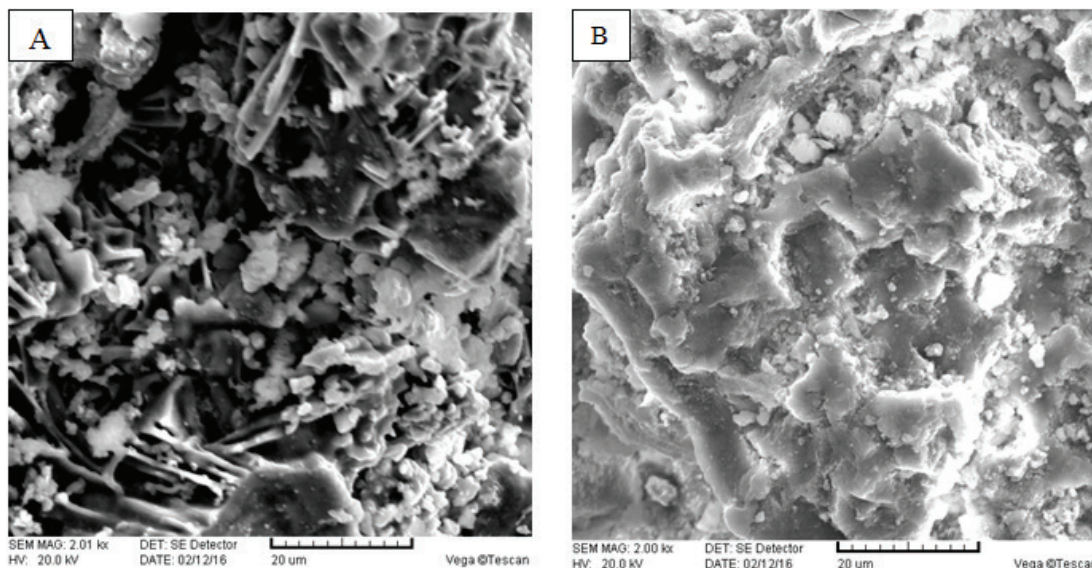


Fig. 3. SEM images of woody biomass fly ash (A) before sorption and (B) after the sorption of the Congo red.

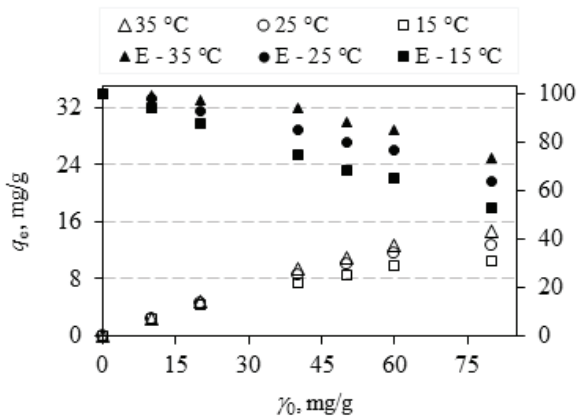


Fig. 5. Effect of the initial dye concentration and temperature on the sorption amount (q_e , mg/g) and efficiency (E , %) of Congo red dye by woody biomass fly ash (WBFA). Condition: m (WBFA) = 200 mg, V (CR) = 50 mL, t = 120 min, T = 25°C.

equilibrium (mg/L), K_F is a constant indicative of the relative sorption capacity of the sorbent ((mg/g)(L/mg) $^{1/n}$) and n describes the isotherm curvature and gives an estimate of the adsorptive intensity.

The linearized form is formulated as follows:

$$\log q_e = \log K_F + \frac{1}{n} \log \gamma_e \quad (4)$$

If the sorption obeys Freundlich Eq. (3), K_F and n can be calculated from the slope and the intercept of the linear $\log q_e$ vs. $\log \gamma_e$ (Fig. 6(A)).

The Langmuir model is applicable for monolayer adsorption. This model assumes that adsorption occurs at specific homogeneous adsorption sites within the sorbent. It is then assumed that once CR molecule occupies a site, no further sorption can take place at that site. It is represented by the following [29]:

$$q_e = \frac{q_m K_L \gamma_e}{1 + K_L \gamma_e} \quad (5)$$

where q_e is the equilibrium adsorption capacity (mg/g), γ_e is the equilibrium liquid phase concentration (mg/L), q_m is the maximum adsorption capacity (mg/g) and K_L is a sorption equilibrium constant (L/mg). The sorption data were analyzed according to the following linear form of Langmuir equation:

$$\frac{\gamma_e}{q_e} = \frac{1}{K_L q_m} + \frac{1}{q_m} \gamma_e \quad (6)$$

The constants (q_m and K_L) were evaluated from the slope and intercept of the straight lines of plot of γ_e/q_e vs. γ_e (Fig. 6(B)).

The essential characteristics of a Langmuir isotherm can be explained in terms of a dimensionless constant, separation factor or equilibrium parameter (R_L) [30], which is represented as follows:

$$R_L = \frac{1}{1 + K_L \gamma_0} \quad (7)$$

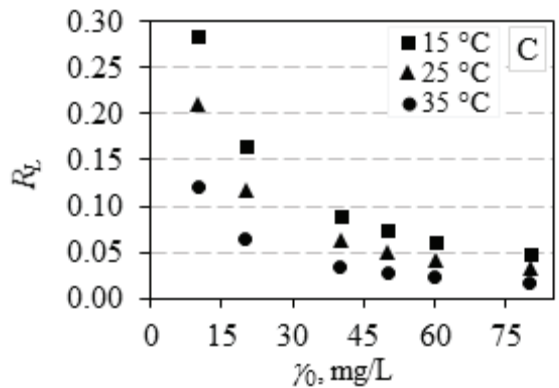
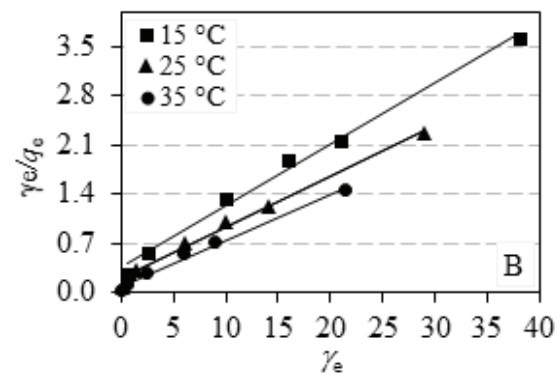
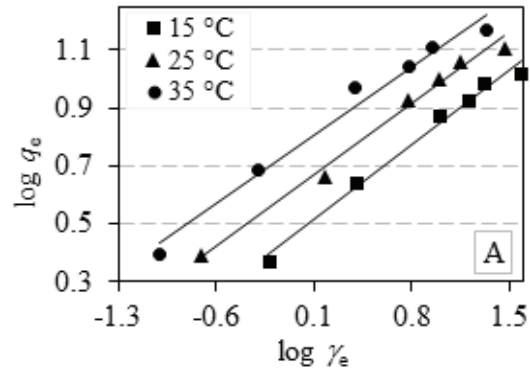


Fig. 6. Sorption of Congo red dye on the woody biomass fly ash: (A) the Freundlich isotherm, (B) the Langmuir isotherm and (C) the separation factor values (R_L) against the initial CR dye concentration at different temperatures.

where K_L is Langmuir sorption equilibrium constant (L/mg), γ_0 is the initial concentration of CR in the solution (mg/L). Figs. 6(A) and (B) show the fitted equilibrium data in the Freundlich and Langmuir isotherms. The fitting results, that is, isotherm parameters and the coefficients of determination, R^2 , are shown in Table 3. The magnitude of the exponent n gives an indication of the favourability of sorption. It is generally stated that the n values in the range 2–10 represent good, 1–2 moderately difficult and <1 poor sorption characteristics [18,31,32]. The n values were 2.69, 2.85 and 3.12 at 288, 298 and 308 K, respectively, suggesting the biomass fly ash is the good sorbent for the CR [18,32].

Table 3
Sorption isotherm constants of Congo red dye on woody biomass fly ash

Isotherm	Parameter	T (K)		
		288	298	308
Freundlich	n	2.69	2.85	3.12
	$K_F ((\text{mg/g})(\text{L/mg})^{1/n})$	2.30	4.29	6.132
	R^2	0.9880	0.9896	0.9858
Langmuir	q_m (mg/g)	11.40	13.68	15.27
	K_L (L/mg)	0.252	0.377	0.736
	R^2	0.9925	0.9904	0.9933

It can be seen that the Langmuir isotherm fits the data better than the Freundlich one. This is confirmed by the high value of R^2 in the case of Langmuir (0.9925, 0.9904 and 0.9933) compared with the Freundlich (0.9880, 0.9896 and 0.9858) and this indicates that the sorption of CR on WBFA takes place as a monolayer adsorption on a surface that is homogenous in sorption affinity [32]. The maximum sorption capacities calculated by the Langmuir model were 11.40, 13.68 and 15.27 mg/g at 15°C, 25°C and 55°C, respectively. The value at 25°C was comparable with the sorption capacities (calculated by using the Langmuir model) of sorbents reported in the literature for CR dye removal listed in Table 4.

Plots of the separation factor, R_L against the initial CR dye concentration at the different solution temperatures are shown in Fig. 6(C).

R_L values indicate the type of isotherm to be irreversible ($R_L = 0$), favourable ($0 < R_L < 1$), linear ($R_L = 1$) or unfavourable ($R_L > 1$). The R_L values obtained for CR dye at three different temperatures are < 1 , which indicates that the sorption was favourable at the concentration range studied. The R_L values decreased with the increase in the initial dye concentration. This shows that the sorption process is favourable at higher dye concentration.

3.4. Kinetic modelling

Information on the kinetics of CR sorption is required to select the optimal condition for the full-scale batch CR removal processes. The sorption kinetics depends on the sorbate–sorbent interactions and experimental conditions. The kinetics of CR sorption was investigated by applying the pseudo-first-order and pseudo-second order model. The pseudo-first-order model of Lagergren is described by the following equation [47]:

$$\frac{dq_t}{dt} = k_1(q_e - q_t) \quad (8)$$

where q_e and q_t are the amounts of CR (mg/g) sorbed on sorbent at equilibrium and at time t , respectively, and k_1 (min^{-1}) is the rate constant of the pseudo-first-order sorption. Integrating Eq. (6) with the boundary conditions of $q_t = 0$ at $t = 0$ and $q_t = q_t$ at $t = t$, yields:

$$\ln(q_e - q_t) = \ln q_e - k_1 t \quad (9)$$

Table 4
Comparison of the Langmuir monolayer sorption capacity (q_m , mg/g) for the sorption of CR by non-conventional sorbents

Sorbents	q_m (mg/g)	Reference
Activated carbon (laboratory grade)	1.88	[33]
Chitosan-coated quartz sand	3.56	[34]
Waste red mud	4.05	[35]
Cashew nut shell	5.18	[36]
Activated carbon from coir pith	6.7	[37]
Acid activated red mud	7.09	[26]
Australian kaolins	7.27	[38]
Rubber seeds (<i>Hevea brasiliensis</i>)	9.82	[27]
Bagasse fly ash	11.88	[33]
Biomass fly ash	13.68	Present work
<i>Alternanthera bettzichiana</i> plant powder	14.67	[39]
Tea waste	32.26	[25]
<i>Azadirachta indica</i> (known as the neem tree)	28.3–41.2	[40]
Sugarcane bagasse	38.2	[41]
Cattail root	38.79	[42]
Activated pine cone	40.19	[43]
Pyrolusite reductive leaching residue	45.66	[44]
Jujuba seeds	55.56	[45]
Eucalyptus wood	66.6	[46]
(<i>Eucalyptus globulus</i>) sawdust		
Cationic-modified orange peel powder	107	[32]

A plot (Fig. 7(A)) of $\ln(q_e - q_t)$ against t gives $q_e = \exp(\text{intercept})$, $k_1 = -(\text{slope})$.

The kinetic data were further analyzed using the Ho's pseudo-second-order kinetic model. The pseudo-second-order equation is represented as follows [48]:

$$\frac{dq_t}{dt} = k_2(q_e - q_t)^2 \quad (10)$$

where q_e and q_t are the amounts of CR (mg/g) sorbed on the sorbent at the equilibrium and at time t , respectively, and k_2 is the rate constant of the pseudo-second-order sorption (mg/g min). Integrating Eq. (5) for the boundary conditions $q_t = 0$ to $q_t = q_t$ and $t = 0$ to $t = t$, the following equation is obtained:

$$\frac{t}{q_t} = \frac{1}{k_2 q_e^2} + \frac{t}{q_e} \quad (11)$$

A plot (Fig. 7(B)) of t/q_t against t gives $1/q_e$ as the slope and $\frac{q_t}{q_e}$ as the intercept.

The values of q_e , k_1 and R^2 obtained from the linear plots (Fig. 7(A)) of Eq. (9) and q_e , k_2 and R^2 from the plots (Fig. 7(B)) of Eq. (11) for the CR sorption on the biomass fly ash at different initial CR concentration are reported in Table 5.

It can be seen (Table 5) that for the pseudo-first-order model, the linear correlation coefficient (R^2) is less than the

pseudo-second-order correlation coefficient (R^2). The correlation coefficients for the pseudo-second-order kinetic model were very high ($R^2 > 0.99$) and the theoretical $q_{e,cal}$ values were closer to the experimental $q_{e,exp}$ values at all studied initial CR concentrations. This suggests that the sorption of CR on the WBFA might be controlled by a mechanism corresponding to the second-order model. Similar kinetic results have also been reported for the adsorption of CR onto the orange peel powder [32], rubber seeds [27], tea waste [25] and cationic-modified orange peel powder [32].

3.5. Sorption mechanism

As the two abovementioned kinetic models could not definitely reveal the sorption mechanism as well as the

rate-controlling steps of the sorption process, intraparticle diffusion model according to Weber and Morris [49] was also applied. The intraparticle diffusion equation is expressed as follows:

$$q_t = k_{pi} \sqrt{t} + C_i \tag{12}$$

where k_{pi} (mg/g min^{1/2}), the rate parameter of stage i , is obtained from the slope of the straight line of q_t vs. $t^{1/2}$. C_i , the intercept of stage i , gives an idea about the thickness of boundary layer, that is, the larger the intercept, the greater the boundary layer effect. If the intraparticle diffusion occurs, then q_t vs. $t^{1/2}$ will be linear and if the plot passes through the origin, then the rate-limiting process is only due to the intraparticle diffusion. Otherwise, some other mechanism along with intraparticle diffusion is also involved. For a sorbate/sorbent sorption process, the sorbate transfer may include the step of either external mass transfer (film diffusion) or intraparticle diffusion, or both. The intraparticle diffusion plots of q_t against $t^{1/2}$ (Fig. 8) consist of three linear sections with different slopes, which indicate that multiple steps take place during sorption process [50].

The first stage of sorption (section of the curve with a large slope) corresponds to transport of sorbate from the bulk solution to the external surface of sorbent by film diffusion, which is also called outer diffusion (or boundary layer diffusion). The second stage of sorption describes the gradual adsorption stage, corresponding to the diffusion of the sorbate from the external surface into the pores of the sorbent. This is called intraparticle diffusion or inner diffusion. The third stage with

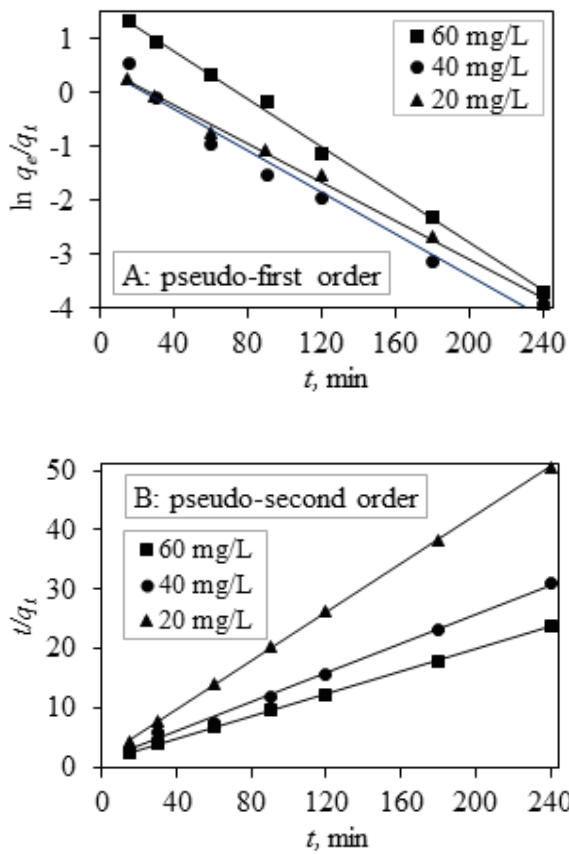


Fig. 7. Sorption of Congo red dye on woody biomass fly ash (A) pseudo-first order plots and (B) pseudo-second order plots.

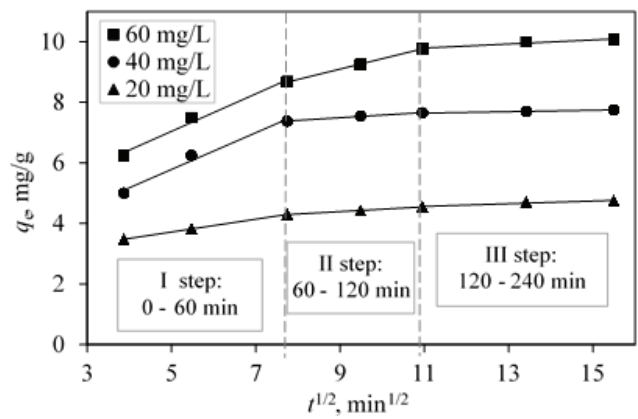


Fig. 8. Plot of intraparticle diffusion model for the sorption of Congo red dye onto woody biomass fly ash at 25°C.

Table 5

The pseudo-first-order and the pseudo-second-order sorption models' constants for the Congo red sorption on woody biomass fly ash

γ_0 (mg CR/L)	$q_{e,exp}$ (μ g/g)	Kinetic model					
		Pseudo-first-order			Pseudo-second-order		
		k_1 (1/min)	$q_{e,cal}$ (mg/g)	R^2	k_2 (g/mg min)	$q_{e,cal}$ (mg/g)	R^2
20	4.77	0.018	1.65	0.9945	0.025	4.89	0.9998
40	7.77	0.020	1.47	0.9426	0.029	7.91	0.9999
60	10.1	0.023	5.39	0.9979	0.008	10.6	0.9997

a small slope indicates the final equilibrium stage: this step is considered to be very fast and thus cannot be treated as the rate-controlling step. Generally, the sorption rate is controlled by outer diffusion (film diffusion) or intraparticle diffusion or both. It is clear from Fig. 8 that the rate-controlling step of CR dye sorption on WBFA involves complex processes, including outer diffusion (film diffusion) and the intraparticle diffusion. The model parameters obtained from the three stages of plots are listed in Table 6. It can be observed from Table 6 that the values of the intercept increased with the initial concentration, which implies that the thickness of the boundary layer increased by increasing the initial concentration.

According to the intraparticle diffusion model, if the value of C is zero, it means that the rate of sorption is controlled by the intraparticle diffusion for the whole sorption period. For all initial concentrations of CR dye, the values of C for each linear stage are not zero (Table 6), indicating that the intraparticle diffusion was present as a part of the diffusion process, but it is not the only rate-controlling step in all stages [51]. Additionally, q_t vs. $t^{1/2}$ should be linear if the intraparticle diffusion was involved in the sorption process. This shows that the sorption processes were not only conducted by intraparticle diffusion, but also by film diffusion, which played a role in the observed processes [52]. In order to determine the actual rate-controlling steps of sorption of CR dye onto WBFA, the experimental data were further analyzed by the Boyd model [53] using the following expression:

$$Bt = -0.4977 - \ln(1 - F) \quad (13)$$

where Bt is a mathematical function of F , F is determined from q_t/q_e . Then, the plots of Bt vs. t are used to find out whether the process is film or particle diffusion controlled. The rate-controlling step is pore diffusion if this plot is linear and passes through the origin. If the plot is non-linear or linear but does not pass through the origin, surface (film) diffusion is the rate-controlling step [52,54]. The Bt vs. t plot is presented in Fig. 9. The plots are linear and do not pass through the origin (the intercepts are all non-zero), indicating that external mass transfer (surface film diffusion) mainly governs the sorption process. A similar observation was previously reported for the adsorption of CR from aqueous solution over the tea waste [25] and cattail root [42].

3.6. Sorption thermodynamics

Thermodynamic parameters are used for better understanding of the effect of temperature on CR dye sorption

on BFA sorbent. The thermodynamic parameters including changes of Gibbs free energy (ΔG°), the enthalpy (ΔH°) and entropy (ΔS°) for the sorption of CR by BFA were determined by using the following equations [55,56]:

$$\Delta G^\circ = -RT \ln(K^\circ) \quad (14)$$

$$K^\circ = K_L \times M_{\text{adsorbate}} \times 1,000 \times 55.5 \quad (15)$$

$$\ln K^\circ = -\frac{\Delta H^\circ}{RT} + \frac{\Delta S^\circ}{R} \quad (16)$$

where K° is dimensionless standard equilibrium constant, K_L is Langmuir sorption equilibrium constant (L/mg), $M_{\text{adsorbate}}$ is the molar mass (g/mol) of adsorbate (CR), 55.5 is the number of moles of pure water per liter, 1,000 (1 dm³ = 1,000 mL (or g, since the solution density is \approx 1 g/mL)), T is the temperature in K and R stands for the universal gas constant (8.314 J/mol K). ΔH° and ΔS° were obtained from the slope and the intercept of the plots of $\ln K^\circ$ vs. $1/T$ (Fig. 10). The calculated thermodynamic parameters for CR sorption on BFA are listed in Table 7.

Negative values of Gibbs free energy (ΔG°) suggest the feasibility of sorption process. Obtained values of Gibbs free energy (ΔG°) decrease with the increasing temperature which indicates the spontaneity of the process at higher temperatures [18,25,32]. The endothermic nature was also confirmed from the positive values of enthalpy change (ΔH°), while good affinity of CR towards the sorbent materials is revealed

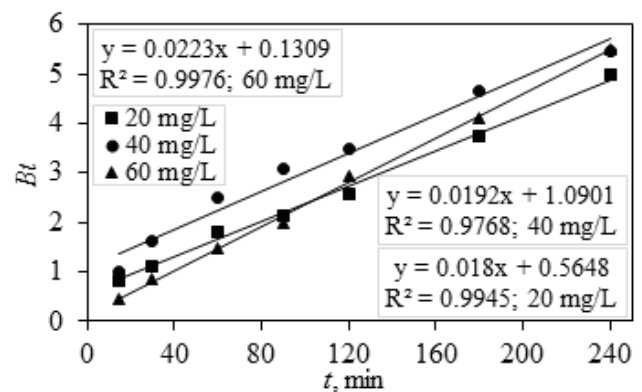


Fig. 9. Boyd plots (Bt vs. t) for the sorption of CR onto the WBFA at three different temperatures.

Table 6

Intraparticle diffusion model constants and correlation coefficients for sorption of Congo red dye on woody biomass fly ash

γ_0 (mg/L)	Intraparticle diffusion								
	First stage of sorption			Second stage of sorption			Third stage of sorption		
	k_{p1} (mg/g min ^{1/2})	C_1	R^2	k_{p2} (mg/g min ^{1/2})	C_2	R^2	k_{p3} (mg/g min ^{1/2})	C_3	R^2
20	0.213	2.65	0.9999	0.078	3.69	0.9976	0.045	4.07	0.9472
40	0.605	2.76	0.9834	0.086	6.72	0.9886	0.022	7.41	0.9970
60	0.619	3.95	0.9865	0.343	9.06	0.9995	0.067	9.06	0.9472

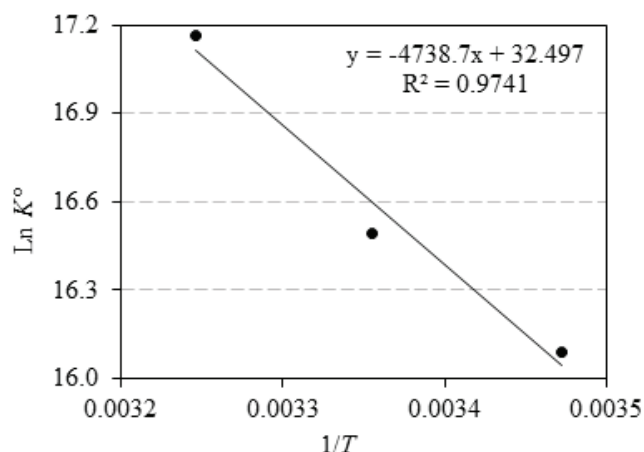


Fig. 10. Plot of $\ln K^\circ$ vs. $1/T$ for the estimation of the thermodynamic parameters for the sorption of CR onto BFA.

Table 7
Thermodynamic parameters for CR sorption onto BFA

Temperature (K)	ΔG° (kJ/mol)	Regression results		
		ΔH° (kJ/mol)	ΔS° (kJ/mol K)	R^2
288	-38.53			
298	-40.87	39.40	0.27	0.9741
308	-43.95			

by the positive value of entropy change (ΔS°). The endothermic adsorption has also been reported for the adsorption of CR on cattail root [42], tea waste [25], jujuba seed [45] and cationic-modified orange peel powder [32].

4. Conclusions

In this study, biomass fly ash was tested and evaluated as a possible sorbent for the removal of ionic, toxic and carcinogenic diazo dye (CR) from its aqueous solution. Experiments were performed by means of the batch sorption technique. The sorption studies were carried out as a function of the contact time, the initial CR dye concentration and temperature. On the basis of the obtained results, the following conclusion can be drawn:

- It was found that the CR dye removal increases with the increase of the agitation time, initial concentration and temperature of CR.
- The sorption of CR onto WBFA was better fitted by the Langmuir than the Freundlich model.
- The values of the dimensionless equilibrium parameters – the separation factor (R_L ; for different temperatures) indicates the favourability of the process described in the present study.
- The kinetic results of the CR sorption on the biomass fly ash were best described by the pseudo-second-order kinetic model.
- The intraparticle plots showed the multilinear curves, which indicated that more than one adsorption

mechanism is involved in the adsorption process. The sorption of CR dye on biomass fly ash occurs through the combination of the film and intraparticle mechanism.

- The negative value of the Gibbs free energy (ΔG°) and the positive value of enthalpy change (ΔH°) indicated that the sorption of CR onto BFA is spontaneous and endothermic. The positive value of entropy change (ΔS°) shows that randomness increases at the solid/liquid interface during the sorption of CR aqueous solution onto BFA.

The present findings suggest that the biomass fly ash can be used as a non-conventional sorbent for the removal of CR dye from aqueous solutions.

References

- [1] M. Rafatullah, O. Sulaiman, R. Hashim, A. Ahmad, Adsorption of methylene blue on low-cost adsorbents; a review, *J. Hazard. Mater.*, 177 (2009) 70–80.
- [2] K.P. Shinde, P.R. Thorat, Biodecolorization of diazo direct dye congo red by *Fusarium* sp. TSF-01, *Rev. Res.*, 2 (2013) 1–7.
- [3] N. Nasuha, B.H. Hameed, Adsorption of methylene blue from aqueous solution onto NaOH-modified rejected tea, *Chem. Eng. J.*, 166 (2011) 783–786.
- [4] G. Crini, Non-conventional low-cost adsorbents for dye removal: a review, *Bioresour. Technol.*, 97 (2006) 1061–1085.
- [5] S. Mondal, Methods of dye removal from dye house effluent—an overview, *Environ. Eng. Sci.*, 25 (2008) 383–396.
- [6] R. Kaur, H. Kaur, Electrochemical degradation of Congo red from aqueous solution: role of graphite anode as electrode material, *Portugaliae Electrochim. Acta*, 34 (2016) 185–196.
- [7] L. Fan, Y. Zhou, W. Yang, G. Chen, F. Yang, Electrochemical degradation of aqueous solution of Amaranth azo dye on ACF under potentiostatic model, *Dyes Pigm.*, 76 (2008) 440–446.
- [8] M.Z.B. Mukhlis, M.M.R. Khan, A.R. Islam, A.N.M.S. Akanda, Removal of reactive dye from aqueous solution using coagulation–flocculation coupled with adsorption on papaya leaf, *J. Mech. Eng. Sci.*, 10 (2016) 1884–1894.
- [9] T. Puspasari, K.V. Peinemann, Application of thin film cellulose composite membrane for dye wastewater reuse, *J. Water Process Eng.*, 13 (2016) 176–182.
- [10] K.P. Gopinath, K. Muthukumar, M. Velan, Sonochemical degradation of Congo red: optimization through response surface methodology, *Chem. Eng. J.*, 157 (2010) 427–433.
- [11] V. Marinović, D. Ljubas, L. Ćurković, Effects of concentration and UV radiation wavelengths on photolytic and photocatalytic degradation of azo dyes aqueous solutions by sol-gel TiO_2 films, *Holistic Approach Environ.*, 7 (2017) 3–14.
- [12] D. Ljubas, L. Ćurković, S. Dobrović, Photocatalytic degradation of an azo dye by UV irradiation at 254 and 365 nm, *Trans. FAMENA*, 34 (2010) 19–28.
- [13] A.M.S. Solano, S. Garcia-Segura, C.A. Martínez-Huitile, E. Brillas, Degradation of acidic aqueous solutions of the diazo dye Congo Red by photo-assisted electrochemical processes based on Fenton's reaction chemistry, *Appl. Catal., B*, 168–169 (2015) 559–571.
- [14] J.C. Cardoso, G.G. Bessegato, M.V. Boldrin Zanoni, Efficiency comparison of ozonation, photolysis, photocatalysis and photoelectrocatalysis methods in real textile wastewater decolorization, *Water Res.*, 98 (2016) 39–46.
- [15] I. Cretescu, T. Lupascu, I. Buciscanu, T. Balau-Mindru, G. Soreanu, Low-cost sorbents for the removal of acid dyes from aqueous solutions, *Process Saf. Environ. Prot.*, 108 (2017) 57–66.
- [16] M. Rožić, I. Senji, S. Miljanić, Methylene blue sorption characterisation onto orange and lemon peels, *Holistic Approach Environ.*, 4 (2014) 97–110.
- [17] F. Deniz, S. Karaman, Removal of Basic Red 46 dye from aqueous solution by pine tree leaves, *Chem. Eng. J.*, 170 (2011) 67–74.

- [18] D. Pathania, A. Sharma, Z.M. Siddiqi, Removal of congo red dye from aqueous system using *Phoenix dactylifera* seeds, *J. Mol. Liq.*, 219 (2016) 359–367.
- [19] M. Auta, B.H. Hameed, Modified mesoporous clay adsorbent for adsorption isotherm and kinetics of methylene blue, *Chem. Eng. J.*, 198–199 (2012) 219–227.
- [20] K.S. Chou, J.C. Tsai, C.T. Lo, The adsorption of Congo red and vacuum pump oil by rice hull ash, *Bioresour. Technol.*, 78 (2001) 217–219.
- [21] M. Abbas, M. Trari, Kinetic, equilibrium and thermodynamic study on the removal of Congo Red from aqueous solutions by adsorption onto apricot stone, *Process Saf. Environ.*, 98 (2015) 424–436.
- [22] K. Rastogi, J.N. Sahu, B.C. Meikap, M.N. Biswas, Removal of methylene blue from wastewater using fly ash as an adsorbent by hydrocyclone, *J. Hazard. Mater.*, 158 (2008) 531–540.
- [23] M.R.R. Kooh, L.B.L. Lim, L.H. Lim, M.K. Dahri, Separation of toxic rhodamine B from aqueous solution using an efficient low-cost material, *Azolla pinnata*, by adsorption method, *Environ. Monit. Assess.*, 188 (2016) 1–15.
- [24] S. Banerjee, G.C. Sharma, R.K. Gautam, M.C. Chattopadhyaya, S.N. Upadhyay, Y.C. Sharma, Removal of Malachite Green, a hazardous dye from aqueous solutions using *Avena sativa* (oat) hull as a potential adsorbent, *J. Mol. Liq.*, 213 (2016) 162–172.
- [25] M. Foroughi-Dahr, H. Abolghasemi, M. Esmaili, A. Shojamoradi, H. Fatoorehchi, Adsorption characteristics of Congo Red from aqueous solution onto tea waste, *Chem. Eng. Commun.*, 202 (2015) 181–193.
- [26] A. Tor, Y. Gengelglu, Removal of congo red from aqueous solution by adsorption onto acid activated red mud, *J. Hazard. Mater.*, 138 (2006) 409–415.
- [27] M.A. Zulfikar, H. Setiyanto, Rusnadi, L. Solakhudin, Rubber seeds (*Hevea brasiliensis*): an adsorbent for adsorption of Congo red from aqueous solution, *Desal. Wat. Treat.*, 56 (2015) 2976–2987.
- [28] H.M.F. Freundlich, Over the adsorption in solution, *J. Phys. Chem.*, 57 (1906) 385–471.
- [29] I. Langmuir, The constitution and fundamental properties of solids and liquids, *J. Am. Chem. Soc.*, 38 (1916) 2221–2295.
- [30] K.R. Hall, L.C. Eagleton, A. Acrivos, T. Vermeulen, Pore- and solid-diffusion kinetics in fixed-bed absorption under constant-pattern conditions, *Ind. Eng. Chem. Fundam.*, 5 (1966) 212–223.
- [31] M. Hadi, M.R. Samarghandi, Equilibrium two-parameter isotherms of acid dyes sorption by activated carbons: study of residual errors, *Chem. Eng. J.*, 160 (2010) 408–416.
- [32] V.S. Munagapati, D.S. Kim, Adsorption of anionic azo dye Congo Red from aqueous solution by cationic modified orange peel powder, *J. Mol. Liq.*, 220 (2016) 540–548.
- [33] I.D. Mall, V.C. Srivastava, N.K. Agarwal, I.M. Mishra, Removal of Congo red from aqueous solution by bagasse fly ash and activated carbon: kinetic study and equilibrium isotherm analyses, *Chemosphere*, 61 (2005) 492–501.
- [34] T. Feng, F. Zhang, J. Wang, L. Wang, Application of chitosan-coated quartz sand for congo red adsorption from aqueous solution, *J. Appl. Polym. Sci.*, 125 (2012) 1766–1772.
- [35] C. Namasivayam, D.J.S.E. Arasi, Removal of congo red from wastewater by adsorption onto waste red mud, *Chemosphere*, 34 (1997) 401–417.
- [36] P. Senthil-Kumar, S. Ramalingam, C. Senthamarai, M. Niranjanna, P. Vijayalakshmi, S. Sivanesan, Adsorption of dye from aqueous solution by cashew nut shell: studies on equilibrium isotherm, kinetics and thermodynamics of interactions, *Desalination*, 261 (2010) 52–60.
- [37] C. Namasivayam, D. Kavitha, Removal of congo red from water by adsorption onto activated carbon prepared from coir pith, an agricultural solid waste, *Dyes Pigm.*, 54 (2002) 47–58.
- [38] V. Vimonses, S. Lei, B. Jin, C.W.K. Chow, C. Saint, Adsorption of congo red by three Australian kaolins, *Appl. Clay Sci.*, 43 (2009) 465–472.
- [39] A.K. Patil, V.S. Shrivastava, *Alternanthera bettzichiana* plant powder as low cost adsorbent for removal of Congo red from aqueous solution, *Int. J. Chem. Tech. Res.*, 2 (2010) 842–850.
- [40] K.G. Bhattacharyya, A. Sharma, *Azadirachta indica* leaf powder as an effective biosorbent for dyes: a case study with aqueous Congo red solutions, *J. Environ. Manage.*, 71 (2004) 217–229.
- [41] Z. Zhang, L. Moghaddam, I.M. O'Hara, W.O.S. Doherty, Congo red adsorption by ball milled sugarcane bagasse, *Chem. Eng. J.*, 178 (2011) 122–128.
- [42] Z. Hu, H. Chen, F. Ji, S. Yuan, Removal of Congo Red from aqueous solution by cattail root, *J. Hazard. Mater.*, 173 (2010) 292–297.
- [43] S. Dawood, T.K. Sen, Removal of anionic dye Congo red from aqueous solution by raw pine and acid-treated pine cone powder as adsorbent: equilibrium, thermodynamic, kinetics, mechanism and process design, *Water Res.*, 46 (2012) 1933–1946.
- [44] W. Shen, B. Liao, W. Sun, S. Su, S. Ding, Adsorption of Congo red from aqueous solution onto pyrolusite reductive leaching residue, *Desal. Wat. Treat.*, 52 (2014) 3564–3571.
- [45] M.C. Somasekhara Reddy, L. Sivaramkrishna, A. Varada Reddy, The use of an agricultural waste material, Jujuba seeds for the removal of anionic dye (Congo red) from aqueous medium, *J. Hazard. Mater.*, 203–204 (2012) 118–127.
- [46] V.S. Mane, P.V. Vijay Babu, Kinetic and equilibrium studies on the removal of Congo red from aqueous solution using Eucalyptus wood (*Eucalyptus globulus*) sawdust, *J. Taiwan Inst. Chem. Eng.*, 44 (2013) 81–88.
- [47] S. Langergren, B.K. Svenska, Zur theorie der sogenannten adsorption geloeester stoffe, *K. Sven. Veternsk.akad. Handl.*, 24 (1898) 1–39.
- [48] Y.S. Ho, G. McKay, The kinetics of sorption of basic dyes from aqueous solutions by sphagnum moss peat, *Can. J. Chem. Eng.*, 76 (1998) 822–826.
- [49] W.J. Weber, J.C. Moris, Kinetics of adsorption on carbon from solution, *J. Sanit. Eng. Div.*, 89 (1963) 31–60.
- [50] P. Janoš, V. Šmídová, Effects of surfactants on the adsorptive removal of basic dyes from water using an organomineral sorbent-iron humate, *J. Colloid Interface Sci.*, 291 (2005) 19–27.
- [51] M. Toor, B. Jin, Adsorption characteristics, isotherm, kinetics, and diffusion of modified natural bentonite for removing diazo dye, *Chem. Eng. J.*, 187 (2012) 79–88.
- [52] K. Vasanth Kumar, V. Ramamurthi, S. Sivanesan, Modeling the mechanism involved during the sorption of methylene blue onto fly ash, *J. Colloid Interface Sci.*, 284 (2005) 14–21.
- [53] G.E. Boyd, A.W. Adamson, L.S. Myers Jr., The exchange adsorption of ions from aqueous solutions by organic zeolites. II. Kinetics, *J. Am. Chem. Soc.*, 69 (1947) 2836–2848.
- [54] Y. Önal, C. Akmil-Basar, C. Sarıcl-Özdemir, Investigation kinetics mechanisms of adsorption malachite green onto activated carbon, *J. Hazard. Mater.*, 146 (2007) 194–203.
- [55] X. Zhou, X. Zhou, The unit problem in the thermodynamic calculation of adsorption using the Langmuir equation, *Chem. Eng. Commun.*, 201 (2014) 1459–1467.
- [56] H.N. Tran, S.J. You, H.P. Chao, Thermodynamic parameters of cadmium adsorption onto orange peel calculated from various methods: a comparison study, *J. Environ. Chem. Eng.*, 4 (2016) 2671–2682.